

# Benefits of Superconducting Technology to Wireless CDMA Networks

M. I. Salkola, *Member, IEEE*, and D. J. Scalapino

**Abstract**—Compact high-temperature superconducting filters have high selectivity and sensitivity. Combined with a cryocooled low-noise amplifier, they significantly reduce the effective noise factor of a cellular base-station receiver. Their impact on wireless code-division multiple-access networks is examined using an analytical analysis and numerical simulations. Potential benefits of the superconducting technology include increased capacity utilization and coverage efficiency. Numerical simulations also address the question of how the network should be optimized to realize these benefits.

**Index Terms**—Code division multiaccess, high-temperature superconductors, intermodulation distortion, wireless network modeling and simulation.

## I. INTRODUCTION

THE RAPIDLY growing demands for wireless communications stress the capabilities of existing systems and the designs of future systems. To meet this challenge, advanced network signal processing algorithms and new hardware are being developed. One new hardware development is the use of thin-film high-temperature superconductors (HTS<sup>2</sup>) and cryocooled low-noise amplifiers (LNAs) to reduce the system noise factor of wireless base-station receivers [1], [2]. In this paper, we examine the potential benefits that this hardware can bring to a code-division multiple-access (CDMA) network.

The basic function of the cryocooled receiver front end, which contains the HTS filter and the LNA, is to remove out-of-band-signal power and amplify in-band signals with a minimum degradation of the signal-to-noise ratio. The reduction in the system noise factor of the base-station receiver associated with the introduction of the HTS front end arises from three factors. First, the decrease in the insertion loss and the lower operating temperature of the HTS filter significantly lowers the noise factor of the filter. Second, the LNA operating in the cryogenic environment adds only a small amount of noise, and its gain effectively eliminates the in-band noise contribution from the rest of the receiver. Third, the high selectivity of the HTS filter removes out-of-band signals, which would typically generate intermodulation distortion (IMD) noises due to the nonlinearities in the rest of the receiver chain and increase the effective noise factor of the receiver.

Manuscript received September 29, 2004; revised August 11, 2005. The review of this paper was coordinated by Prof. B. Li.

M. I. Salkola is with the Superconductor Technologies Inc., Santa Barbara, CA 93111 USA.

D. J. Scalapino is with the Department of Physics, University of California, Santa Barbara, CA 93106 USA.

Digital Object Identifier 10.1109/TVT.2005.863471

For the purposes of the CDMA benefit analysis, the properties of the cryocooled front end can be characterized by the effective noise factor  $F$  of the base-station receiver [3]. This is directly measurable as the CDMA analysis shows that, for a given situation, the decibel reduction of the noise factor is equal to the decibel reduction in the mobile power when the HTS unit is put in place.<sup>1</sup> Thus, other things being equal, an HTS system will reduce mobile transmit power leading to longer battery life. More generally, for systems that are reverse-link<sup>2</sup> limited, the deduction in the mobile transmit power can be traded off for other network improvements: Both the analytical and numerical simulations show that the HTS unit increases capacity utilization for a given coverage, increases coverage for a given capacity utilization, fills coverage holes, and enables higher reverse-link data transmission rates. The numerical simulations also show the benefits of HTS' in reducing call blocking and dropping as well as the need for a proper optimization of the network to realize these benefits.

In this paper, we extend our earlier work on HTS benefits that also examined the preliminary experimental evidence for the theory [3]. In addition to deriving an analytical theory for describing the effect of nonlinear receivers, we develop a novel real-time approach for quantifying the performance of wireless CDMA networks in the presence of IMD noises and other imperfections. In particular, we can now determine various quality-of-service metrics that include service availability and reliability. Our performance analysis shows that the intermodulation response of present base-station receivers can reduce the capacity of a network considerably. The HTS front end lowers the effective noise factor of the receiver and improves the quality of service of the network, which is manifested by fewer dropped and blocked calls. While there can be many reasons for the network to drop calls, important RF causes affecting the reverse link include out-of-band interference and the near-far problem. They are eliminated by the use of HTS front ends.

We begin in Section II by generalizing the conventional definition of the noise factor so that it also takes into account the nonlinear noise generated in a base-station receiver. It is the reduction in the effective (generalized) noise factor of the receiver that determines the benefit of the HTS system. In Section III, we consider the CDMA capacity in the presence of fluctuations that arise from the fact that power control is not perfect, an IMD noise can be present, and the offered traffic is

<sup>1</sup>The noise figure (in decibels) is defined as  $NF = 10 \lg F$ , where  $F$  is the noise factor. Note that dBm is a unit of power in decibels with respect to 1 mW.

<sup>2</sup>The reverse link refers to the mobile to base-station link and the forward link to the base station to mobile link.

a random process. In Sections IV–VI, we turn to a discussion of a numerical simulation that allows us to go beyond the analytical theory and examine the role of the forward link and its effect on the benefits to the network performance that can be realized. Our numerical simulation method shows its strength when analyzing complex systems, in particular, in Section VII where the CDMA network is exposed to IMD noises with different time scales. In the Section VIII, we summarize what our analysis has found regarding the benefits that the superconducting technology brings to wireless CDMA networks. We point out that the numerical simulations support the analytical relationships and provide a way to extend them.

## II. EFFECTIVE NOISE FACTOR

The purpose of an HTS filter is to provide high selectivity with low insertion loss over a desired passband. The high selectivity removes the out-of-band-signal strength that would have been mixed into the band of interest by the nonlinear intermodulation of amplifiers and mixers further down the receiver chain. The low insertion loss means that very little of the desired signal is lost when passing through the filter, and its low operating temperature combined with this low loss implies that only a small amount of thermal noise is added. The low-temperature environment required for the HTS filter can also be used to hold an LNA whose gain mitigates the noise introduced by the remaining part of the receiver chain.

The enhanced performance of a cellular system utilizing an HTS filter and an LNA front end can be characterized in terms of an effective (generalized) noise factor. In addition to accounting for the conventional thermal noise, it includes the IMD noise due to the nonlinear character of the receiver. Defining the conventional noise factor of the receive system as  $F_R$ , the effective noise factor  $F$  of the system becomes

$$F = F_R + \frac{N_{\text{IMD}}}{N_{\text{in}}}. \quad (1)$$

Here,  $N_{\text{in}} = kT_0W$  is the ambient noise power at the input,  $W$  is the channel bandwidth,  $k$  is Boltzmann's constant,  $T_0$  is the standard noise temperature of 290 K, and  $N_{\text{IMD}}$  is the IMD noise power referred to the input of the receiver at a given frequency.

In addition to the steady state intermodulation, which increases the average effective noise factor, power fluctuations in the interfering signals lead to fluctuations in the IMD noise power. Consequently, the IMD noise power can have components characterized by multiple time scales. Therefore, the standard deviation  $\sigma_F$  of the effective noise factor  $F$  can be large. If the CDMA system cannot compensate for these fluctuations fast enough, these fluctuations will have an adverse effect on the system capacity. Highly selective HTS filtering removes both the steady state IMD noise power and its fluctuations so that  $F$  is minimized with  $\sigma_F \simeq 0$ . In particular, the selectivity of the HTS filter is effective in reducing the out-of-band-signal strength that leads to an IMD in the amplifier and the rest of the receiver following the filter. Thus, while  $N_{\text{IMD}}/N_{\text{in}}$  can make a significant contribution to the effective noise factor when conventional filtering is used, the selectivity of the HTS filter

suppresses its contribution to  $F$ . In this case, the effective noise factor  $F$  of the receiver with the HTS front end is close to unity.

## III. REVERSE-LINK CAPACITY AND COVERAGE

On the reverse link, the physical layer is the part of the CDMA communications protocol between the mobile user and the base station that is most affected by the improvements in the sensitivity and the selectivity of the base-station receiver provided by an HTS front end. In this section, we discuss the capacity and coverage benefits provided by an HTS front end.

In practice, an imperfect power control and an IMD noise will result in fluctuating received power at the base-station receiver. Since a CDMA cellular system is interference limited, it does not have a fixed number of channels, as this depends on the amount of interference and the desired quality of service. The statistical nature of available links makes it convenient to define the capacity of the system in terms of a blocking probability. This is the probability that a new user will be denied access to the network. The number of users that can be supported for a given blocking probability is defined to be the soft, or Erlang, capacity of the system.

We assume a call-admission policy where calls are blocked upon arriving, if the total interference  $I$  at a base-station receiver exceeds a certain value  $I_0$ . The blocking probability is

$$B = \text{Prob}(I > I_0) \quad (2)$$

where the total interference is given by

$$I = \sum_i \alpha_i C_i + FN_{\text{in}}. \quad (3)$$

The sum is over all mobile users in the network, including the neighboring cells, and all users are characterized by an average voice-activity factor with the same statistical properties; for example,  $\langle \alpha \rangle = \langle \alpha_i \rangle$ . In general, propagation measurements show that the received carrier power  $C_i$  for the  $i$ th user is a lognormal random variable [4]. Similarly, bit energy-to-noise spectral density ratio is assumed to be a lognormal random variable

$$\left( \frac{E_b}{N_0} \right)_i = \varepsilon_i e^{\sigma_0 z_i}. \quad (4)$$

Here,  $\varepsilon_i$  is the median bit energy-to-noise spectral density value for the  $i$ th mobile user,  $\sigma_0$  is the standard deviation, and  $z_i$  is a random Gaussian variable with a zero mean and a unit standard deviation. We assume that the target  $E_b/N_0$  values are set so that all users have the same median  $E_b/N_0$  value:  $\varepsilon = \varepsilon_i$ .

A new call is blocked, if  $I > I_0$ . The critical interference  $I_0$  is the maximum amount of interference that the network can sustain with a desired quality of service. Most importantly,  $I_0$  determines the coverage area of the network by limiting the total interference to values such that the active users within that area have a high enough probability of maintaining the call. It can be parameterized by a noise factor  $F_0$  and a loading factor  $X_0$  as  $I_0 = F_0 N_{\text{in}} / (1 - X_0)$ . While  $F_0$  could be selected to be the conventional noise factor  $F_R$ , in the presence of an IMD noise, it is convenient to define  $F_0$  as a median value of the

effective noise factor  $F$ . For a constant  $F$ ,  $X_0$  becomes the loading threshold; equivalently, a new call is blocked if the cell loading exceeds the loading threshold  $X_0$ .

Defining the effective noise factor as  $F = F_0(1 + f)$  and  $X_0(f) = X_0 - (1 - X_0)f$ , where  $f$  takes into account the fluctuating IMD noise  $N_{\text{IMD}}$  arising from the nonlinear contribution in (1), the blocking condition can be written as  $\sum_i \alpha_i C_i / I > X_0(f)$ . It can be shown [4]–[6] that, in a Gaussian approximation with Poisson-distributed call traffic, the blocking probability is

$$B(X; f) = \frac{1}{2} \text{Erfc} \left( \frac{X_0(f) - X e^{\frac{\sigma_0^2}{2}}}{\sqrt{2\beta_0 X}} \right). \quad (5)$$

Here,  $X = A/n_\infty$  is the average cell loading, and  $A$  is the average carried traffic per cell.  $A$  and  $X$  define the soft (Erlang) capacity of the system per cell for a given blocking probability. The constant of proportionality

$$n_\infty = \frac{1}{\langle \alpha \rangle (1 + \xi) K} \quad (6)$$

is the limiting theoretical cell capacity: the pole capacity. The parameter  $K = \varepsilon R/W$  is the dimensionless data rate,  $R$  is a given data rate,  $W$  is the spread-spectrum bandwidth of the communication channel, and  $\xi$  is the first-order reuse fraction. The parameter  $\beta_0$  is defined as

$$\beta_0 = \frac{\langle \alpha^2 \rangle}{\langle \alpha \rangle} \left( \frac{1 + \xi'}{1 + \xi} \right) K e^{2\sigma_0^2} \quad (7)$$

where the second-order reuse fraction  $\xi'$  measures the mean-square interference due to users in the other cells. Typical values of  $\xi$  and  $\xi'$  are 0.55 and 0.086, respectively [4].

For a constant effective noise factor, the blocking probability is given by (5). However, the blocking probability increases if the effective noise factor fluctuates, which would be the case when the base-station receiver does not have selective enough filtering. This reduces the capacity of the CDMA system. Let  $p(f)$  be the probability distribution function of  $f$ . Then, the blocking probability becomes

$$B(X) = \int_{-\infty}^{\infty} df p(f) B(X; f). \quad (8)$$

If the time scale of noise-factor fluctuations is much shorter than that of the power control, the power-control accuracy decreases and  $\sigma_0$  in (5) and (7) must be replaced by the actual power-control accuracy  $\sigma > \sigma_0$ . In general,  $B(X)$  can be evaluated exactly by numerical integration. However, if  $f$  is a Gaussian random process, a closed-form result can be derived. Assuming that  $f$  is a Gaussian random variable with zero mean and standard deviation  $\sigma_F$ , the blocking probability is

$$B(X) = \frac{1}{2} \text{Erfc} \left( \frac{X_0 - X e^{\frac{\sigma_0^2}{2}}}{\sqrt{2(\beta_0 X + \beta_F)}} \right) \quad (9)$$

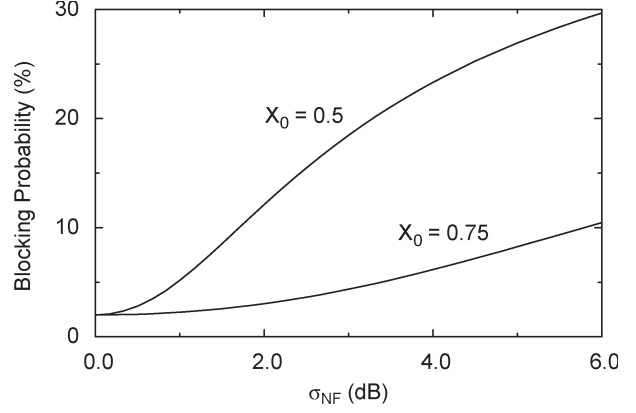


Fig. 1. Blocking probability  $B(X)$  as a function of the standard deviation of the effective noise figure  $\sigma_{\text{NF}} = 10\sigma_F/\ln 10$ , for  $X_0 = 0.5$  and  $0.75$ . The offered traffic  $A_0$  is kept constant while the carried traffic  $A = Xn_\infty$  is determined from the self-consistency condition  $A = A_0[1 - B(X)]$ . The offered traffic is such that, for  $\sigma_F = 0$ , the blocking probability  $B = 2\%$ . The other parameters are  $\sigma_0 = 1.5$  dB,  $\xi = 0.55$ ,  $\xi' = 0.086$ ,  $\langle \alpha \rangle = 0.4$ ,  $\langle \alpha^2 \rangle = 0.31$ , and  $K = 5/128$ .

where  $\beta_F = \sigma_F^2(1 - X_0)^2$ . For  $\sigma_F < \sqrt{\beta_0 X}/(1 - X_0)$ , the blocking probability is only weakly affected by a fluctuating effective noise factor. In contrast, outside this regime, the blocking probability increases rapidly with an increasing  $\sigma_F$ . Note that  $\beta_F$  decreases as  $X_0$  increases. Thus, in an IMD-limited environment, poor filtering can be detrimental to the network capacity. The selectivity provided by an HTS filter eliminates the fluctuation of the effective noise factor and, thus, removes this problem. This effect of fluctuations in the effective noise factor on the blocking probability is illustrated in Fig. 1, for  $X_0 = 0.5$  and  $0.75$ .

Even though the CDMA system does not have a well-defined number of channels, it still features a phenomenon known as “trunking efficiency” in which the soft capacity  $X$  increases more than the increase the loading threshold  $X_0$  would imply. This is a direct consequence of the law of large numbers where the magnitude of fluctuations in the total channel interference grows only as  $\sqrt{X}$ . The capacity can therefore be increased further, because the standard deviation of interference fluctuations is actually decreased in relative terms. Also, since the relative standard deviation of the traffic distribution decreases as the magnitude of the traffic increases, a higher cell loading can be supported for the same blocking probability. However, in a CDMA system, the trunking efficiency would be observed even under deterministic traffic conditions.

Specifically, consider the soft capacity increase when the receiver noise factor or the IMD noise is reduced. For a given blocking probability  $B$  less than 50%, the soft capacity  $X$  is obtained from (9) as

$$X = e^{-\frac{\sigma_0^2}{2}} \left[ X_0 + 2\nu \left( 1 - \sqrt{1 + \frac{X_0}{\nu} + \frac{\beta_F}{\beta_0 \nu} e^{\frac{\sigma_0^2}{2}}} \right) \right] \quad (10)$$

where  $\nu = (1/2)q^2\beta_0 e^{-\sigma_0^2/2}$ , and  $q$  is defined so that  $B = (1/2)\text{Erfc}(q)$ . This result has a number of interesting consequences.

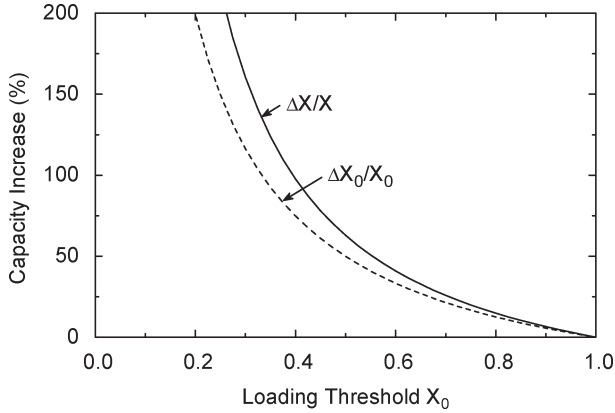


Fig. 2. Relative increase in the loading threshold  $\Delta X_0/X_0$  (dashed line) and the soft capacity  $\Delta X/X$  (solid line) as a function of the loading threshold  $X_0$ , when the noise factor is decreased by a factor of 2 (3 dB). Here,  $B = 2\%$ ,  $\sigma_0 = 1.5$  dB, and  $\sigma_F = 0$ .

First, the capacity is sensitive to the IMD noise. As the magnitude of IMD fluctuations increases, the soft capacity decreases in order to maintain the constant blocking probability. Second, the increase in the soft capacity exceeds that of the loading threshold when the noise factor is reduced. If the noise factor changes from  $F$  to  $F'$ , the relative change in the loading threshold is [3]

$$\frac{\Delta X_0}{X_0} = -\frac{\Delta F}{F} \left( \frac{1 - X_0}{X_0} \right) \quad (11)$$

where  $\Delta F = F' - F$  is the change in the noise factor and  $\Delta X_0 = X'_0 - X_0$  is the allowed change in the loading threshold for a fixed coverage area. However, for a nonzero  $\nu/X_0$ , an increase in the loading threshold will produce a larger increase in the soft capacity. As a practical example, consider  $\nu \ll X_0$ . If we further assume that  $\Delta X_0 \ll X_0$  and  $\sigma_F = 0$ , the relative increase in the soft capacity is

$$\frac{\Delta X}{X} = \left( 1 + \sqrt{\frac{\nu}{X_0}} \right) \frac{\Delta X_0}{X_0} \quad (12)$$

which is larger than the relative increase in the loading threshold  $\Delta X_0/X_0$ . In the limit where  $\nu/X_0 \rightarrow 0$ , the increase in the soft capacity is the same as the increase in the loading threshold.

For a typical situation with  $F/F' = 2$ ,  $X_0 = 0.5$ ,  $B = 2\%$ , and  $\sigma_0 = 1.5$  dB, we obtain  $\nu = 0.027$  and the soft capacity increase determined from (10) is 63%, which is 26% more than that suggested by the increase in the loading threshold in (11). Fig. 2 illustrates the contribution of the trunking efficiency to the actual capacity increase.

Third, network deployments can take advantage of HTS improvements by trading off capacity-utilization and coverage-efficiency benefits. The desired design parameter is often the traffic density, and we must consider whether the number of base stations can be reduced while still serving the same number of users per unit area. Here, we derive the minimum number of base stations required to cover an area with a given uniform user density. The coverage efficiency increases as the noise factor decreases. Note that the coverage efficiency is inversely proportional to the number of base stations per unit area.

The scale for the number of base stations  $N_{BS}$  is set by  $S/\pi\ell_0^2$ , and the scale for the carried number of users  $N$  is set by  $n_\infty e^{-\sigma_0^2/2} (S/\pi\ell_0^2)$ . Here,  $S$  is the coverage area of the network and  $\ell_0$  is the limiting radius of a cell such that a mobile user transmitting from the cell edge would have the required signal-to-noise ratio if there were no other users and the noise factor of the receiver was unity. Since  $\ell_0$  and  $n_\infty$  both depend on the specifics of the system, in the following discussion, it is convenient to work with normalized quantities so that  $\mathcal{N}_{BS} = N_{BS}/(S/\pi\ell_0^2)$  measures the number of base stations relative to  $S/\pi\ell_0^2$  and  $\mathcal{N} = N/(n_\infty e^{-\sigma_0^2/2} S/\pi\ell_0^2)$  measures the number of users relative to  $n_\infty e^{-\sigma_0^2/2} (S/\pi\ell_0^2)$ . We further assume that the propagation exponent governing the signal attenuation as a function of distance is 4 and consider  $\nu \ll 1$ . Thus,  $\mathcal{N} = X_0 \mathcal{N}_{BS}$ .

The coverage efficiency  $1/\mathcal{N}_{BS}$  is determined under the constraint that, for a given user density, the number of base stations is minimized. The coverage area per base station is determined by the loading threshold  $X_0$ . For a given number of users  $\mathcal{N}$ , the number of required base stations becomes

$$\mathcal{N}_{BS} = \left( \frac{2F}{\mathcal{N}} \right) \frac{1}{\sqrt{1 + \frac{4F}{\mathcal{N}^2} - 1}}. \quad (13)$$

Clearly, the coverage efficiency increases as the noise factor decreases. By varying the user density and therefore  $\mathcal{N}$ , the impact of the effective noise factor  $F$  on the size of the network can be found for various situations.

For a small user density,  $\mathcal{N} \ll \sqrt{F}$ , the loading threshold becomes  $X_0 = \mathcal{N}/\sqrt{F}$ , and the number of base stations is proportional to the square root of the noise factor

$$\mathcal{N}_{BS} = \sqrt{F}. \quad (14)$$

If the noise factor is reduced by a certain factor, the number of required base stations decreases by the square root of the same factor. Note that when the user density is small, we get the same result independent of whether the number of users per base station or per unit area is kept constant.

For a large user density,  $\mathcal{N} \gg \sqrt{F}$ , the loading threshold is  $X_0 = 1 - F/\mathcal{N}^2$ , and  $X_0$  approaches 1. In this limit, the number of base stations depends only weakly on the noise factor

$$\mathcal{N}_{BS} = \mathcal{N} \left( 1 + \frac{F}{\mathcal{N}^2} \right). \quad (15)$$

In this case, the cell loading is so close to one that the interference due to the users dominates over the ambient noise, rendering the noise factor of the receiver irrelevant.

#### IV. STATISTICAL MODEL OF A CDMA NETWORK

The CDMA network is an interference-limited system in which the overall system performance relies on balancing the forward and the reverse links. For balanced networks, improvements in the reverse-link performance should be met with similar improvements in the forward direction. These

may include increasing the total transmitted power of the base stations as well as adjusting the soft handoffs.

In this section, we describe a statistical model of a CDMA network that we will study using numerical simulation techniques. The parameters of the model and the nature of the network optimization problem will be discussed. We note that, for this model, the numerical simulation takes into account the fact that the forward-link performance differs from that of the reverse link. These differences, caused by multiple-access interference and soft handoffs, lead to different pole capacities for the forward and the reverse links. Although we use Interim Standard 95 (IS-95), many of our results are not limited to this air interface but apply to a generic CDMA system.

The forward link of IS-95 CDMA includes four different channel types: a continuously transmitted pilot that provides a reference for all users, a continuously transmitted sync channel for base-station identification and timing, paging channels for control information, and traffic channels for voice. The number of traffic channels per cell is assumed to be 62. Typical target  $E_b/N_0$  values for these channels are  $-15$  dB for the pilot,  $6$  dB for the sync and paging channels, and  $7$  dB for the traffic channels—the corresponding processing gains are  $1$ ,  $1024$ ,  $256$ , and  $128$ , respectively [4]. The actual simulation involves only separate pilot and traffic channels, whereas the remaining channels are included in the pilot channel by an overhead factor. Assuming that there is one active paging channel per base station, this factor is  $2$  dB for the above parameter values. Thus, the pilot  $E_b/N_0$  value used in the simulations is  $-13$  dB.

The simulation utilizes a traffic model where calls arrive randomly and uniformly within the cluster area according to a Poisson distribution with rate  $\lambda$ . Call holding times are exponentially distributed with a mean time  $1/\mu$ , where  $\mu$  is the average departure rate. Thus, in a time interval  $\Delta t$ , the average number of arriving calls is  $\lambda\Delta t$ , and the average number of terminations is  $\mu\Delta t$ . The time interval  $\Delta t$  is selected so that on the average one call arrives during the time interval:  $\lambda\Delta t = 1$ . For example, if the offered traffic is  $60$  E and the average call duration  $120$  s,  $\Delta t = 2$  s. Since mobiles adjust their transmit power once in a  $1.25$ -ms interval, the system has enough time to equilibrate between arriving and terminated calls.

If there were no limitations set by the network at equilibrium, the average traffic  $A$  (number of users) carried by the network would equal the offered traffic:  $A = A_0 \equiv \lambda/\mu$ . However, since arriving calls must be denied access to the network if resources are not available and calls would have to be dropped if a sufficient link cannot be maintained, the offered and carried traffic usually differ. At equilibrium

$$A = A_0(1 - B)(1 - D) \quad (16)$$

where  $B$  is the probability to block an arriving call from the network and  $D$  is the probability that a call is dropped.<sup>3</sup> We can also write

$$A = A_0(1 - B_{\text{eff}}) \quad (17)$$

<sup>3</sup>Thus,  $D$  is the ratio of dropped calls to normally terminated and dropped calls.

where the effective blocking probability  $B_{\text{eff}}$  is defined in terms of the blocking probability  $B$  and the dropped-call probability  $D$  as

$$B_{\text{eff}} = B + (1 - B)D. \quad (18)$$

The effective blocking probability can also be interpreted as a metric for the quality of service where a smaller value of  $B_{\text{eff}}$  implies better quality of service.

A base station blocks a new call when there is no channel element available. This form of blocking is called hard blocking [6]. The number of links available for calls depends on the total amount of noise and interference. When the total amount of noise and interference at the input of a base-station receiver exceeds a threshold value, which is set to maintain the desired coverage and dropped-call rate, arriving calls are denied access to the network. This is called soft blocking. It also accounts for mobile users that cannot access the network because a sufficient reverse or forward transmit power to make a connection is not available. An increase in the carried traffic for a given blocking probability indicates an increased capacity, whereas a decrease in the blocking probability for a given carried traffic load implies a better grade of service.

A user is denied access to the network, if the total interference  $I$  at a base station exceeds the critical interference  $I_0$  or if there are no traffic channels available. Each base station determines  $I$  independently and compares it with  $I_0$ , which is chosen so that the desired coverage is achieved with a given quality of service. The critical interference is defined in terms of a loading threshold  $X_0$  as  $I_0 = F_0 N_{\text{in}} / (1 - X_0)$ , where  $F_0$  is the median value of the effective noise factor  $F$ . The capacity is defined in terms of the effective blocking probability  $B_{\text{eff}}$  that includes both hard and soft blocking: Here, it is the number of users  $A_0$  (or  $A$ ) for which the effective blocking probability equals  $2\%$ .

In our numerical simulations, a soft handoff provides a macroscopic diversity where mobile users can simultaneously communicate with more than one base station. In the forward direction, the received signals from the different base stations are combined with maximal-ratio combining. However, in the reverse direction, selection combining is used where the received signal with the highest  $E_b/N_0$  value in the network is selected.

In the simulation, mobiles and base stations adjust their transmit power in finite steps. If the received  $E_b/N_0$  value is less than the target value, the transmit power is increased and vice versa. This procedure and the fact that the received power  $C_i$  is a lognormal random variable result in imperfect power control. For the chosen values used in the simulation, the standard deviation  $\sigma_0$  of the logarithm of the signal-to-total interference ratio  $\ln(C_i/I)$ , measured at the base-station receiver, is  $1.5$  dB. A call is dropped, if the link reliability is less than  $80\%$ , which happens when the received  $E_b/N_0$  is less than the target  $E_b/N_0$  value more than  $20\%$  of the time due to reverse- or forward-transmit-power limitations.

The voice activity is described by a quaternary random process that parallels the natural voice pattern. The probability of a full-rate transmission is  $29.1\%$ , a half-rate transmission

is 3.9%, a 1/4-rate transmission is 7.2%, and 1/8-rate transmission is 59.8%. Thus, in the reverse link, the average voice-activity factor is  $\langle\alpha\rangle = 0.4$  and  $\langle\alpha^2\rangle = 0.31$ . In the forward link, the power-control bit is taken into account, increasing  $\langle\alpha\rangle$  to 0.45.

The simulation tool can employ any propagation model. As an illustration, we use the empirical International Radio Consultative Committee (CCIR) formula, which is the Hata model for a medium-small city [7]. In the simulations shown below, the base-station antenna height is 50 m, the mobile antenna height is 2 m, the carrier frequency is 830 MHz, and 15% of the study area is covered by buildings. While forward channels are transmitted orthogonally, a multipath propagation usually leads to a forward-link interference. Here, we assume that 70% of the transmitted power appears as interference.

### V. NETWORK PERFORMANCE ANALYSIS

To illustrate what one can learn from a numerical simulation, we consider a cluster of three omnidirectional cells that are designed to cover an area of about 100 km<sup>2</sup>. The base stations form an equilateral triangle that is 6 km on a side. The required coverage area of the network is fixed so that mobile users within 4 km from any base station should be served with good quality of service. Setting the cell radius at approximately 4.3 km, the implied margin in the link budget is sufficient to keep the number of dropped calls small for most cases. The mobile noise figure will be taken as 8 dB, and the mobile peak power will be set at 200 mW, which corresponds to 23 dBm. The nominal base-station noise figure without the HTS front end will be taken as 5 dB. The superconducting front end has the ability to decrease the base-station noise figure down to 2 dB, where the residual noise figure is determined mainly by the antenna, cables, and connectors before the HTS receiver. The capacity of the network is measured for a constant effective blocking probability of approximately 2%. The data was collected over 50 000 time intervals.<sup>4</sup> In this section and in the next, we assume for a moment that the IMD noise is static with  $\sigma_F = 0$ .

Figs. 3 and 4 summarize the simulation results. Without the HTS front end, limiting the loading threshold  $X_0$  to 0.5 allows the cluster to cover the desired area. The three-site cluster can handle an offered traffic of 54 E for the specified effective blocking probability. This corresponds to an average carried traffic of 53 E. The dropped-call probability  $D$  is 0.2%. A sufficient forward-link coverage and soft capacity is obtained when the pilot power is 1 W, and the available total base-station transmit power is 11 W.

With the HTS front end, the loading threshold  $X_0$  can now be increased to 0.75 while maintaining the same required coverage area. For  $B_{\text{eff}} = 2\%$ , the offered traffic can be increased to  $A_0 = 93$  E. The average carried traffic  $A$  is 91 E, and the dropped-call probability  $D$  is 0.3%. The forward link does not limit the capacity of the cluster if the pilot power is increased to 1.3 W, and the maximum base-station transmit power is increased to 25 W. Thus, a 3-dB reduction in the base-station

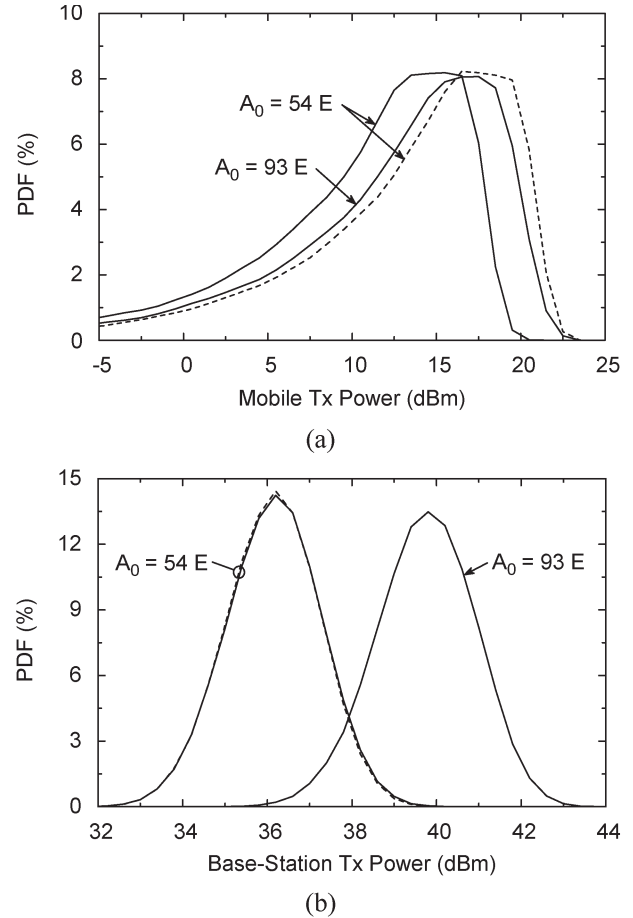


Fig. 3. Probability distribution function of (a) mobile transmit power and (b) total base-station transmit power when the base-station receiver noise figure is 5 dB (dashed line) and 2 dB (solid lines). Without the HTS front end ( $NF = 5$  dB), the offered traffic  $A_0$  is 54 E, the reverse-link loading threshold  $X_0$  is 0.5, and the pilot power is 1 W. With the HTS front end ( $NF = 2$  dB), the offered traffic  $A_0$  is 93 E, the reverse-link loading threshold  $X_0$  is 0.75, and the pilot power is 1.3 W. As a comparison, also shown is the probability distribution function for  $NF = 2$  dB,  $A_0 = 54$  E,  $X_0 = 0.5$ , and a pilot power of 1 W. The distributions are calculated using numerically simulated histograms such that the widths of each power interval are (a) 1 dBm and (b) 0.4 dBm.

receiver noise figure can yield a 75% increase in the voice capacity for the given coverage area, provided the pilot power is increased to 1.3 W, and the base-station transmit power is increased to 25 W.

The “measured” probability distribution functions for the mobile and base-station transmit powers are given in Fig. 3. If the base-station noise figure is reduced by 3 dB but the loading threshold  $X_0$  and the effective blocking probability  $B_{\text{eff}}$  are kept the same, the soft capacity of the network will remain the same. However, the number of dropped calls will vanish and the probability distribution function of the mobile transmit power will shift by 3 dB to lower power levels, as shown in Fig. 3(a). The average mobile transmit power in this simulation was also reduced by 3 dB. Note that even if the loading threshold is also increased to facilitate the capacity increase, the probability distribution functions remain essentially the same as they were for the lower threshold without the HTS front end.

The shape of the probability distribution function for the mobile transmit power shown in Fig. 3(a) can be understood by the fact that the transmit power cannot exceed the peak power

<sup>4</sup>For  $A_0 = 60$  E and the average call duration of 2 min, this would correspond to 28 h of data collection in a real-world network.

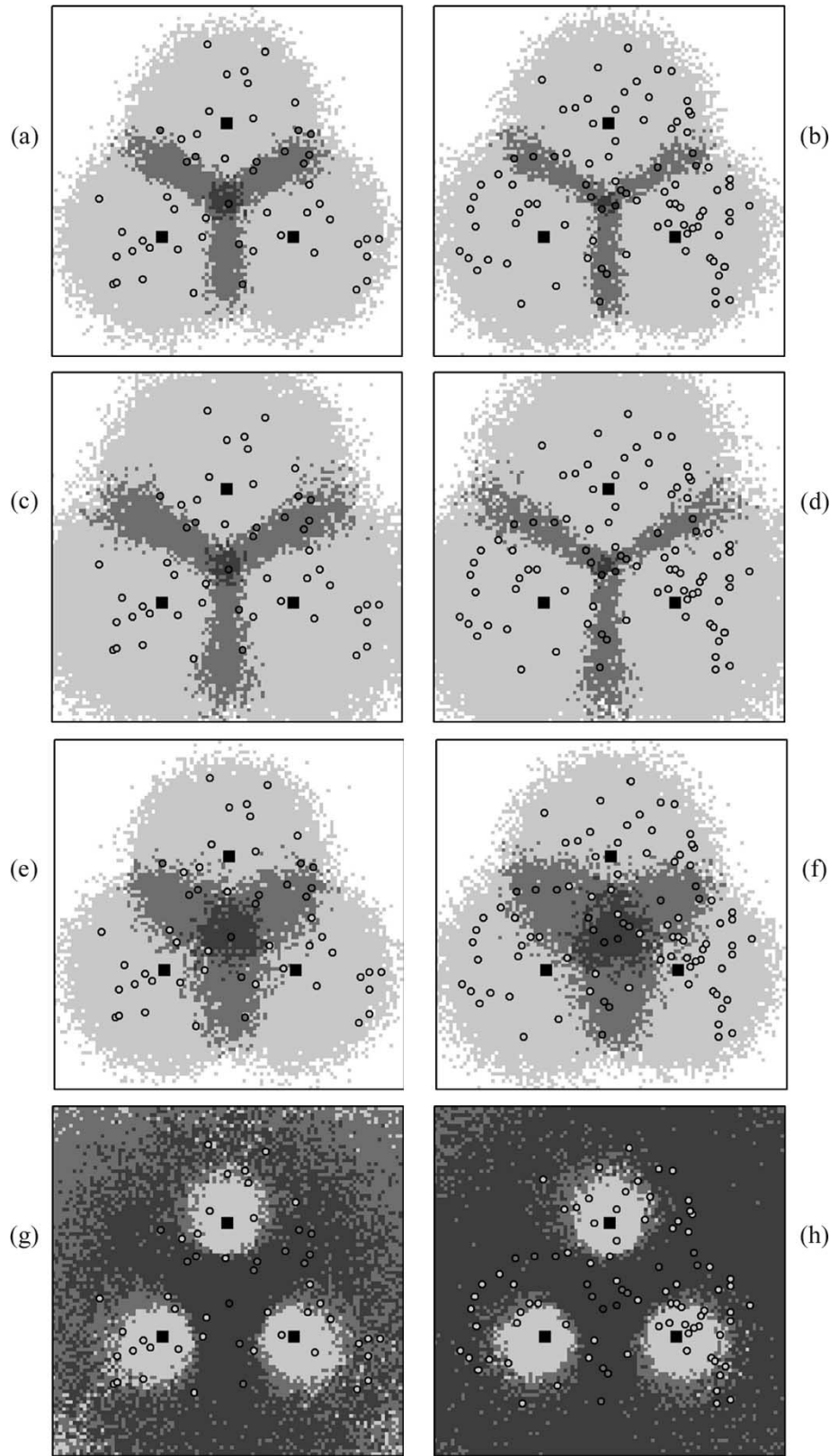


Fig. 4. Instantaneous coverage areas, indicating the appropriate soft-handoff regions for adding a new user, when the base-station receiver noise figure NF is 5 dB, and the number of mobile users is 53 (without HTS filters) and when NF is 2 dB and the number of mobile users is 91 (with HTS filters). Composite coverage area for (a) NF = 5 dB and (b) NF = 2 dB. Pilot coverage area for (c) NF = 5 dB and (d) NF = 2 dB. Reverse coverage area for (e) NF = 5 dB and (f) NF = 2 dB. Forward coverage area for (g) NF = 5 dB and (h) NF = 2 dB. Base stations are denoted by black squares, and mobiles are denoted by filled circles with the gray-color scale indicating the soft-handoff state. White color shows no coverage, light-gray color shows the one-way soft-handoff region, medium-gray color shows the two-way soft-handoff region, and dark-gray color shows the three-way soft-handoff region. The area shown is  $16 \times 16$  km, and the distance between the base stations is 6 km. As noted in the text, in order for the forward link not to limit the increased capacity associated with the HTS front end, one needs to increase the pilot power from 1 to 1.3 W and the maximum base-station transmit power from 11 to 25 W.

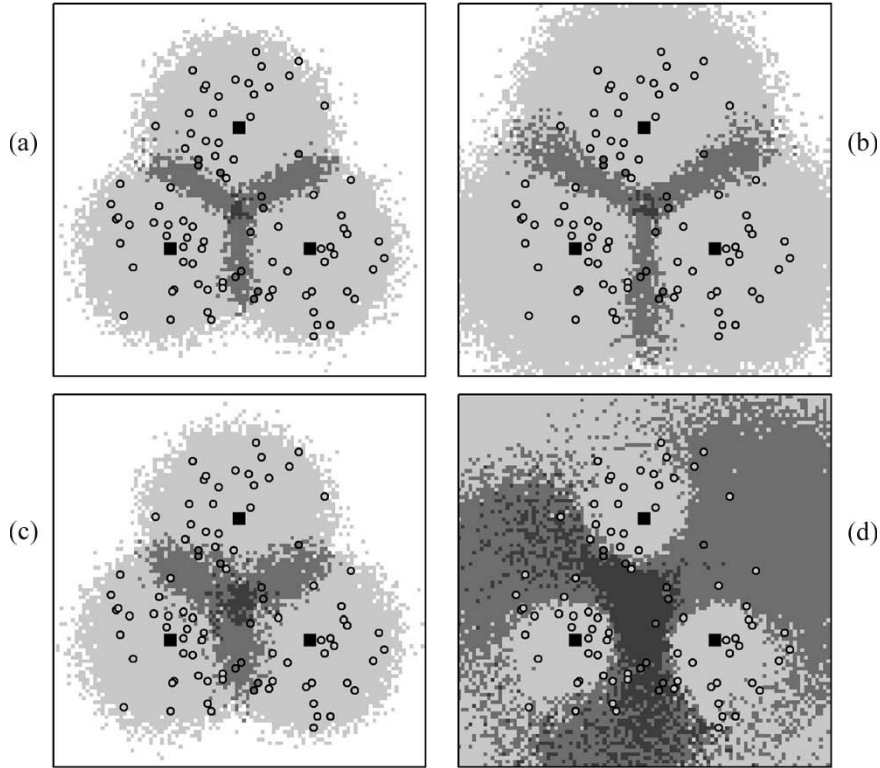


Fig. 5. Instantaneous coverage areas, indicating the appropriate soft-handoff regions for adding a new user, when the base-station receiver noise figure NF is 5 dB, and the number of mobile users is 91. (a) Composite coverage area. (b) Pilot coverage area. (c) Reverse coverage area. (d) Forward coverage area. Base stations are denoted by black squares, and mobiles are denoted by filled circles with the gray-color scale indicating the soft-handoff state. White color shows no coverage, light-gray color shows the one-way soft-handoff region, medium-gray color shows the two-way soft-handoff region, and dark-gray color shows the three-way soft-handoff region. The area shown is  $16 \times 16$  km, and the distance between the base stations is 6 km. The pilot power is 1 W, and the maximum base-station transmit power 11 W.

of 23 dBm (200 mW). At low power levels, the probability distribution function is determined by the mobiles close to the base stations. The differential probability of having mobiles at a distance  $r$  from the base station is  $dP \propto r dr$  in which case their transmit power in dBm units is  $C = 10 \lg r + \text{const}$ . Thus, the probability distribution follows a curve that has the simple form:  $dP/dC \propto 10^{C/(5\gamma)}$ .

Fig. 3(b) illustrates the probability distribution function for the base-station transmit power. Initially, the average base-station transmit power is 36.3 dBm (4.3 W), and the standard deviation is at 1.1 dB. With increased traffic loading, the average base-station transmit power is increased by 3.6 dB, while the standard deviation remains the same. Similarly, the peak transmit power increases by 3.6 dB from 40.4 dBm (11 W) to 44 dBm (25 W). In order to manage the increased reverse-link capacity, the power-handling capabilities of the base stations must be increased by more than a factor of two to ensure that the forward link does not limit the system capacity. As long as the amount of traffic and the coverage area remain the same, reducing the receiver noise factor has no effect on the base-station transmit power. The probability distribution functions are broadened mainly because of variations in the number and the location of mobile users.

Fig. 4 shows the mobile-user locations at one random instant of time with 53 and 91 users and the corresponding coverage areas. For the increased capacity, the reverse-link coverage area is the same, as are the pilot and the composite ones. The

forward-link coverage for traffic is larger for 91 users, because the base-station transmit power was increased so that the unevenly distributed loading conditions and large loadings can be handled without the forward link limiting the capacity. Note the slightly reduced two- and three-way soft-handoff regions in the composite and the pilot plots.

The effect of cell breathing is illustrated in Fig. 5, which shows the coverage areas for the three-site cluster without the HTS front ends when there are 91 users present. Clearly, the reverse and the forward coverage areas are smaller than those with the HTS front ends and with 91 users, shown in Fig. 4. The pilot coverage area is less sensitive to the number of users with the exception that the two- and three-way soft-handoff regions have shrunk.

## VI. NETWORK PLANNING AND CAPACITY

The capacity utilization of the network is determined by the distance between base stations and the propagation loss. Frequently, the capacity utilization can be increased by sectorization and cell splitting. We have shown that reducing the system noise factor will lead to a similar result but that this improvement is sensitive to the cell loading that the network is designed for. In the following discussion, we consider the case in which the locations of base stations are constrained. Similar constraints may be imposed on the antenna height, forcing the network to have a particular loading threshold. We discuss the

increase in capacity associated with an HTS front end and compare the analytic results with the simulation.

The capacity utilization of the cluster network and the capacity increase due to the HTS front end is strongly influenced by the loading threshold, which is a function of base-station antenna height. As the antenna height is increased, the propagation loss decreases, allowing the use of larger loading thresholds; see Fig. 6. For a given loading threshold  $X_0$  and a blocking probability, the average cell loading  $X$  and the concomitant capacity increase can be estimated analytically from (10) and also computed from the numerical simulation.

The main reasons for the deviation between the numerical simulation and the analytical results are soft handoff and blocked and dropped calls, which are dynamically taken into account by the simulation. These are more likely to occur when the number of users  $N$  in the network is high. It is particularly important to realize that blocked and dropped calls will reduce the probability of having high  $N$  values. In fact, numerically obtained probability distribution functions of  $N$  are approximately Gaussian distributed with a standard deviation less than  $\sqrt{A}$ , where  $A = \langle N \rangle$  is the average value of  $N$ .

For the purpose of comparing the numerical simulation with the analytical results, let  $N_k$  denote the instantaneous number of users in a soft-handoff state with the  $k$ th cell's base station ( $k = 1, \dots, N_{\text{BS}}$ ). As a generalization, the instantaneous loading  $X_k$  of the  $k$ th cell is defined so that the instantaneous noise rise relative to the average thermal noise floor  $\langle F \rangle N_{\text{in}}$  at the  $k$ th base station is  $(1 - X_k)^{-1}$ . Furthermore, assume that the number of users in the soft handoff with the  $k$ th base station and its cell loading are linearly related as

$$X_k = \frac{N_k}{n_\infty} \quad (19)$$

where the factor of proportionality  $n_\infty$  defines the pole capacity. It is convenient to write (19) in the form

$$\frac{1}{N_{\text{BS}}} \sum_{k=1}^{N_{\text{BS}}} X_k = \left( \frac{N}{N_{\text{BS}}} \right) \left( \frac{\eta}{n_\infty} \right). \quad (20)$$

The soft-handoff factor  $\eta$  measures the channel overhead due to soft handoffs and is given by

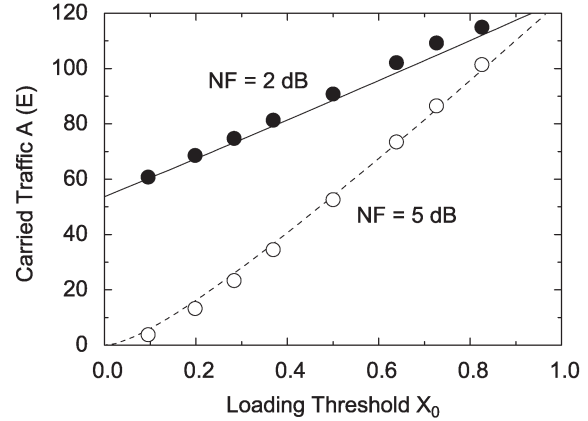
$$\eta = \frac{1}{N} \sum_{k=1}^{N_{\text{BS}}} N_k. \quad (21)$$

For a wide range of values of carried traffic  $A$ , the ratio  $\eta/n_\infty$  is independent of  $N$ , and we can approximate

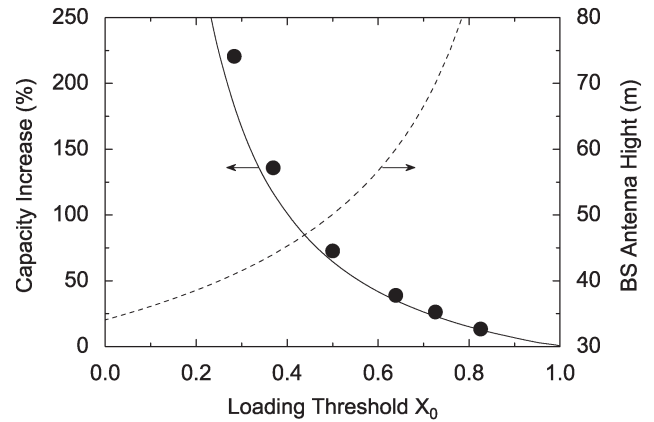
$$X \simeq \left( \frac{A}{N_{\text{BS}}} \right) \left\langle \frac{\eta}{n_\infty} \right\rangle. \quad (22)$$

Here, the average cell loading  $X = \langle X_k \rangle$ . In the analytical theory, the above definition of  $n_\infty$  reduces to (6), for  $\eta = 1$ .

We note in passing that the random variables  $N$ ,  $1/n_\infty$ , and  $\eta$  are approximately Gaussian distributed and exhibit a variable degree of cross correlation. While  $\eta$  and  $1/n_\infty$  are moderately negatively correlated with  $N$ , the ratio  $\eta/n_\infty$  shows only a



(a)



(b)

Fig. 6. (a) Average carried traffic  $A$  as a function of the loading threshold  $X_0$  for base-station receiver noise figures  $NF = 2$  dB (filled circles and solid line) and 5 dB (open circles and dashed line). (b) Corresponding capacity increase  $\Delta X/X$  (filled circles and solid line) and the base-station antenna height as a function of  $X_0$  (dashed line). Quantitative numerical values of  $A$  and  $\Delta X/X$  are computed by simulation (circles) for  $B_{\text{eff}} = 2\%$ , and their corresponding analytical values (lines) are obtained from (10) for  $B = 2\%$ ,  $\sigma_0 = 1.5$  dB,  $\xi = 0.095$ , and  $\xi' = 0.029$ .<sup>5</sup>

small amount of correlation with  $N$ . Thus, for the considered three-site network, (22) is well obeyed with  $\langle \eta/n_\infty \rangle^{-1}$  equal to 50.8. Furthermore, for  $A_0 = 54$  E,  $\langle \eta \rangle = 1.24$ , and  $\langle 1/n_\infty \rangle^{-1} = 63.4$ .

In contrast, the analytical approach postulates a Poisson-distributed-traffic load and uses  $\eta = 1$ . If all arriving calls were admitted to the network and no calls were dropped, the numerically obtained traffic distribution would be Poisson distributed as well. However, the adopted call-admission policy changes the carried traffic distribution to one that is better described as Gaussian with a standard deviation about 8% smaller than  $\sqrt{A}$ . To account for the increased  $A$  due to the modified traffic distribution, we increase the analytical pole capacity by 9%. Thus, in the analytical theory,  $n_\infty = 63.4$  for  $\xi = 0.095$ . This correction does not affect the capacity-increase estimates.

The numerical and analytical results on the capacity increase due to the HTS front end are in good agreement, adding confidence to our conclusions. At high loading threshold

<sup>5</sup>The reuse fractions  $\xi$  and  $\xi'$  are estimated for two adjacent cells using results presented in [4].

values  $X_0$ , the simulation predicts a smaller capacity increase because of the increased forward multiuser interference and because the carried traffic is large enough for hard blocking to occur more often. These effects are also neglected in the analytical treatment.

VII. EFFECT OF AN IMD NOISE ON THE NETWORK PERFORMANCE

As discussed in Section III, fluctuations in the strength of the out-of-band signals lead to IMD-driven fluctuations in the effective noise factor. These degrade the performance of the network. The numerical simulation allows one to treat this problem by dynamically taking into account the time scale of these fluctuations. Here, we conclude our simulation study of the three-site cluster by examining the effect of an IMD noise on the blocking and dropped-call probabilities.

In the following, we assume that the effective noise factor of the base-station receiver is a lognormal random process

$$F = F_0 e^{\sigma_F x} \tag{23}$$

where  $x$  is a Gaussian random process with zero mean and a unit standard deviation.<sup>6</sup> The mean and the standard deviation of the noise figure  $NF = 10 \lg F$  are  $\langle NF \rangle = 10 \lg F_0$  and  $\sigma_{NF} = 10\sigma_F / \ln 10$ , respectively. We will consider two limiting scenarios in which the time scale of  $x$  is either slow or fast relative to the reverse-link power control. In the former case, the system adiabatically follows the noise-factor fluctuations so that the network always maintains an equilibrium state. While the quality of service, as measured by the link quality, is not affected by slow noise-factor fluctuations, the probability of dropped calls can increase drastically because all mobile users associated with a given base station are collectively affected by these fluctuations resulting in occasional large coverage holes. In the latter case, noise-factor fluctuations are too fast for the power control to follow. This causes an additional broadening of the reverse link  $E_b/N_0$ , because mobile users effectively follow the average value of  $C/I$  due to slow power control. In order to maintain the same level of quality of service, the target value of  $E_b/N_0$  must be increased when the network is exposed to fast IMD fluctuations.

First, consider an isolated omnidirectional cell serving randomly distributed mobile users in close proximity to the base station so that the link reliability is not limited by the maximum mobile transmit power. Thus, in this scenario, there are no dropped calls. As an initial design principle, the offered traffic is chosen so that the blocking probability is 2% when there is no IMD noise. This procedure offsets the difference between the call-admission schemes that the analytical and numerical simulations use to manage arriving calls. In contrast to the analytical approach, the numerical simulation discards the blocked calls that cause the offered and carried traffic distributions to differ. The numerical simulation yields  $A_0 = 21 E$  for  $X_0 = 0.5$ .

In the presence of IMD noises, the blocking probability is calculated by a numerical simulation and from (8) for a cell

<sup>6</sup>The results remain essentially the same when the effective noise factor is  $F = F_0 e^{\sigma_F x}$  for  $x > 0$  and  $F = F_0$  for  $x \leq 0$ .

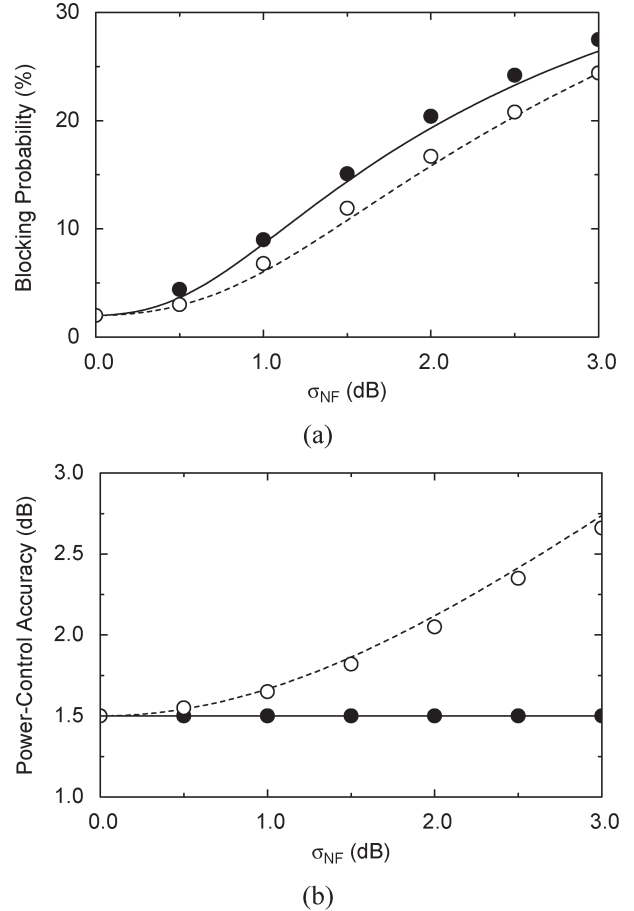


Fig. 7. (a) Blocking probability and (b) reverse power-control accuracy, as measured by the standard deviation of the received  $E_b/N_0$ , as a function of the standard deviation  $\sigma_{NF}$  of the IMD noise for one isolated omnidirectional cell. Here, the propagation loss is given by the CCIR model, the loading threshold  $X_0 = 0.5$ , the average base-station receiver noise figure  $\langle NF \rangle = 5$  dB, and  $\sigma_0 = 1.5$  dB. Simulation and analytical results for slow IMD fluctuations are shown by filled circles and the solid lines and, for fast IMD fluctuations, by open circles and the dashed lines.

loading  $X$  such that

$$A = A_0 [1 - B(X)] \tag{24}$$

where the carried traffic is  $A = X n_\infty$ . Numerically and analytically obtained blocking probabilities are compared in Fig. 7(a), which shows good agreement both for slow and fast IMD fluctuations. As the standard deviation of the IMD noise increases, the probability of blocking a new call increases rapidly, reducing the capacity of a cell.

Fig. 7(b) shows both the analytically and the numerically calculated power-control accuracies, which are defined as the standard deviation of the reverse link  $E_b/N_0$ . While slow IMD fluctuations have no effect on the accuracy of power control, fast IMD fluctuations reduce the accuracy because of the time-scale difference. The effect of fast IMD fluctuations on the power-control accuracy can be estimated by noting that the standard variance of  $E_b/N_0$  is a sum of the intrinsic variance  $\sigma_0^2$  and the standard variance  $\sigma_I^2$  of the total interference (3)

$$\sigma^2 = \sigma_0^2 + \sigma_I^2. \tag{25}$$

For  $A \gg 1$ ,  $\sigma_I$  is same as the standard deviation of the interference variable

$$z_I = \ln \left[ X e^{\frac{\sigma_0^2}{2}} + (1 - X) e^{\sigma_F x} \right] \quad (26)$$

where the multiuser interference is replaced by its average value. For  $\sigma_F < 1$  ( $\sigma_{NF} < 4$  dB), an asymptotic estimate for  $\sigma_I$  can be derived, where

$$\sigma_I = \sigma_F \left( 1 + \frac{X}{1 - X} e^{\frac{\sigma_0^2}{2}} \right)^{-1}. \quad (27)$$

This formula is also exact for any  $\sigma_F$ , when  $X = 0$  or 1. Thus, as the time scale of IMD fluctuations shortens, the standard deviation of  $E_b/N_0$  increases and the accuracy of power control decreases.

With IMD fluctuations, the probability distribution of received power levels  $C$  at a base-station receiver is also lognormal. However, in contrast to the reverse link  $E_b/N_0$ , the standard deviation of  $\ln(C/N_{in})$  decreases when the time scale of IMD fluctuations shortens. For slow IMD fluctuations, the standard deviation of  $\ln(C/N_{in})$  is  $\sqrt{\sigma_0^2 + \sigma_F^2}$ . For fast IMD fluctuations,  $C$  is decoupled from the instantaneous noise factor and depends only on its average value. Therefore, the standard deviation of  $\ln(C/N_{in})$  is reduced approximately to  $\sigma_0$ . This phenomenon, where the fluctuations in the received power levels is reduced to its intrinsic value in the limit of fast IMD fluctuations, is similar to the ‘‘motional narrowing’’ observed in many physical systems where external fluctuations are too fast for a system under consideration to follow [8].

Then, we consider a situation in which the three-site cluster previously introduced in Section V is exposed to IMD noises, described by (23). The simulation results are summarized in Fig. 8 for a reverse-link call-admission policy with  $X_0 = 0.5$  and for  $A_0 = 54$  E. Even with multiple cells and a soft handoff, the numerical and the analytical blocking probabilities are in fair agreement. Slow IMD fluctuations cause the main deviation in the blocking probability through the increased number of dropped calls, because the network is designed for a particular user distribution and capacity assuming that no IMD noise exists. The network is less sensitive to fast IMD fluctuations, as demonstrated by the low dropped-call probability; see Fig. 8(b).

Finally, assume that no call-admission policy on the reverse link has been implemented by setting  $X_0 = 1$ . This scenario is frequently encountered in practice where networks base their admission of arriving calls only on the availability of forward-link resources. We further assume that the standard deviation of the IMD noise is fixed to  $\sigma_{NF} = 2.2$  dB but that the offered traffic is varied. We consider three types of networks: networks of which base-station receivers are exposed to IMD noises and have  $NF = 5$  dB, networks with receivers that are able to eliminate IMD noise but still have  $NF = 5$  dB, and networks of which receivers are so selective and sensitive that the IMD noise is absent and  $NF = 2$  dB. As Fig. 9 demonstrates, the capacity and the quality of service of the network are improved by both eliminating the IMD noise and reducing the noise figure by 3 dB.

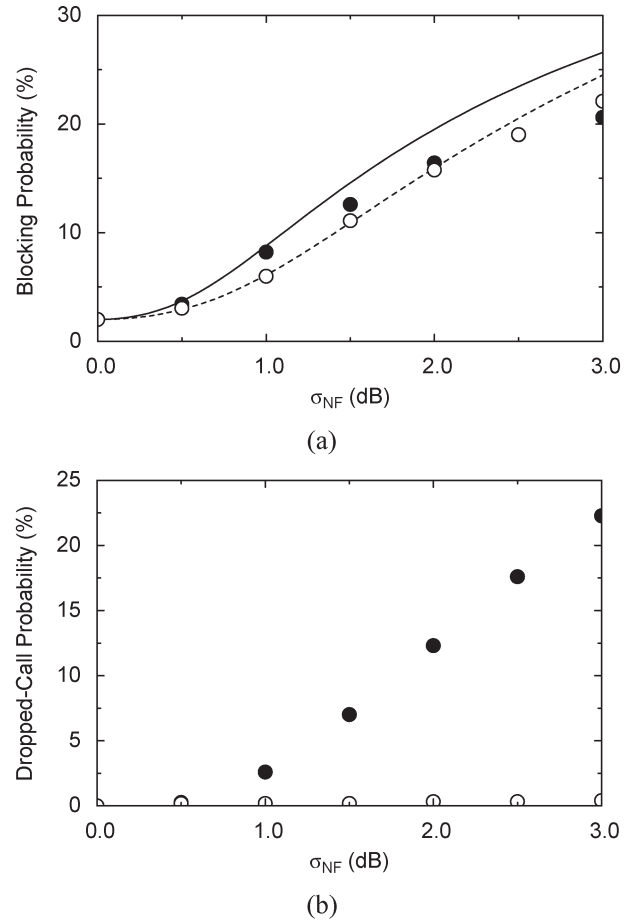


Fig. 8. (a) Blocking probability and (b) dropped-call probability as a function of the standard deviation  $\sigma_{NF}$  of the IMD noise for a network with three omnidirectional cells. The propagation loss is given by the CCIR model, the loading threshold  $X_0 = 0.5$ , the average base-station receiver noise figure  $\langle NF \rangle = 5$  dB,  $\sigma_0 = 1.5$  dB,  $\xi = 0.095$ , and  $\xi' = 0.029$ . Simulation and analytical results for slow IMD fluctuations are shown by filled circles and the solid line and, for fast IMD fluctuations, by open circles and the dashed line.

Either the blocking probability or the dropped-call probability can be used to define the network capacity. The effective blocking probability (18) is a particularly weighted measure of the quality of service and is also suitable for this purpose. Ideally, in networks that use well-defined call-admission policies to maintain an adequate quality of service, calls are dropped only rarely and the blocking probability is used to define the capacity of a network. Here, however, existing calls are being dropped before the blocking probability becomes large, and the effective blocking probability is mainly determined by the dropped-call probability. Note that mobile users unable to connect to the network because of either insufficient reverse or forward transmit power are accounted for as blocked calls.

Defining the capacity as the offered traffic for which the dropped-call probability is 2%, we can conclude from Fig. 9 that, in this particular example, the capacity of the network utilizing sensitive and selective base-station receivers characterized by  $NF = 2$  dB and  $\sigma_{NF} = 0$  is 105 E. This is to be contrasted with the behavior of the system without the HTS front end. In this case, in the presence of IMD noises, the capacity is only 15–42 E, depending on the time scale of IMD fluctuations. The capacity increase due to selectivity and

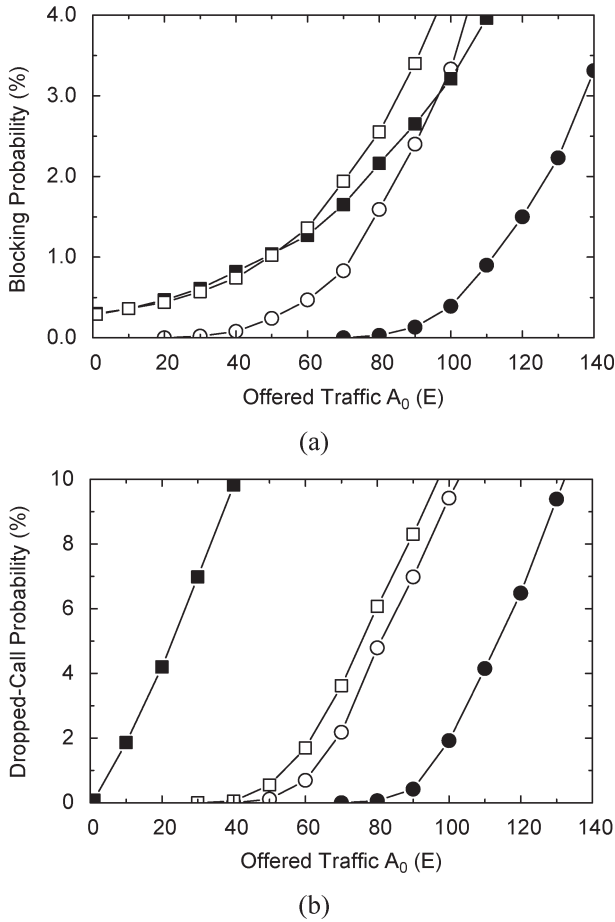


Fig. 9. (a) Blocking probability and (b) dropped-call probability as a function of the offered traffic  $A_0$  for a network with three omnidirectional cells. The propagation loss is given by the CCIR model [7], the loading threshold  $X_0 = 1$ , and  $\sigma_0 = 1.5$  dB. Shown are simulation results for slow IMD fluctuations with  $\langle NF \rangle = 5$  dB and  $\sigma_{NF} = 2$  dB (filled squares), for fast IMD fluctuations with  $\langle NF \rangle = 5$  dB and  $\sigma_{NF} = 2$  dB (open squares), for  $\langle NF \rangle = 5$  dB and  $\sigma_{NF} = 0$  (open circles), and for  $\langle NF \rangle = 2$  dB and  $\sigma_{NF} = 0$  (filled circles).

sensitivity ranges from 150% to 600%. If the receiver is only selective but not sensitive so that  $NF = 5$  dB and  $\sigma_{NF} = 0$ , the capacity of the network is 73 E. This corresponds to a 74–390% increase in the capacity relative to the nonselective base-station receivers in the presence of IMD noises. In the absence of IMD noises, a 3-dB decrease in the base-station will approximately increase the capacity utilization by 44%.

An interesting aspect of the three-cell network analyzed in Fig. 9 is that the effect of an IMD noise on the accuracy of reverse-link power control is obtained using (25) and (27). As it is apparent in Fig. 10, the analytical theory quantitatively explains the numerical simulation results for slow and fast IMD noise fluctuations. Thus, the adverse impact of the imperfect power control on the quality of service and the capacity utilization can be determined.

We conclude this section by noting that because the reverse link of certain third generation systems is conceptually similar to that of IS-95, our findings should apply to these systems as well. The accuracy of power control in the presence of an IMD noise is one relevant example with important implications for any spread-spectrum system.

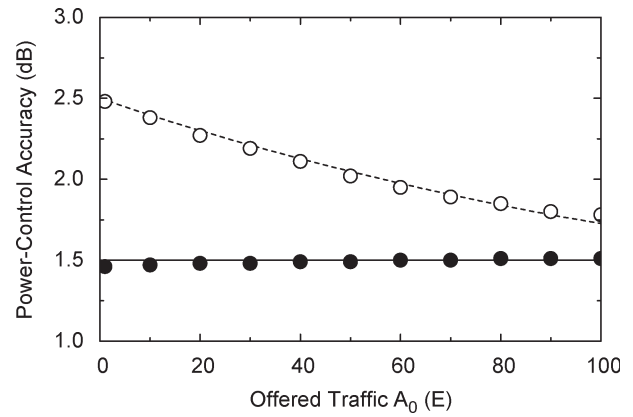


Fig. 10. Reverse power-control accuracy, as measured by the standard deviation of the received  $E_b/N_0$ , as a function of the offered traffic  $A_0$  for a network with three omnidirectional cells. The propagation loss is given by the CCIR model [7], the loading threshold  $X_0 = 1$ , the average base-station receiver noise figure  $\langle NF \rangle = 5$  dB,  $\sigma_{NF} = 2$  dB, and  $\sigma_0 = 1.5$  dB. Simulation and analytical results for slow IMD fluctuations are shown by filled circles and the solid line and, for fast IMD fluctuations, by open circles and the dashed line.

### VIII. FINAL REMARKS

Superconducting (HTS) filters and cryocooled LNAs provide new base-station receiver hardware with enhanced out-of-band interference protection and in-band amplification with exceptionally low degradation of the in-band signal-to-noise ratio. Here, we have investigated the benefits that this technology brings to the reverse link in wireless CDMA networks.

The key parameter characterizing the benefit of superconducting technology is the reduction in the effective noise factor  $\Delta F$  of the base-station receiver when the HTS-LNA front end replaces the conventional front end. A direct measure of  $\Delta F$  is the decibel reduction in mobile transmit power when the HTS-LNA front end is inserted. With other network factors remaining constant, this change in the transmit power provides a simple and robust measure of this important parameter. In reverse-link-limited situations with  $X_0 \sim 0.5$ , a 3-dB decrease in the base-station receiver noise figure will approximately increase the voice capacity utilization by 50%. Additional benefits are increased coverage efficiency or a reduction in the number of required base stations. In out-of-band interference-limited situations, the reduction in the effective noise factor can be larger than 3 dB, leading to enhanced benefits from HTS filtering.

While many of the other predictions depend on details of the model such as the way in which the propagation and the fading is modeled, the trends with changes in  $\Delta F$  provide insight into the effectiveness of an HTS-LNA subsystem on a CDMA network. In general, such relationships are model-dependent; however, there are several results that have a more universal form and, like the measurement of  $\Delta F$ , should be robust. In particular, the relative increase in loading threshold  $\Delta X_0/X_0$  given in (11) is such a relation. If the noise factor  $F$  of the existing base-station receiver is known, a measurement of the change in mobile power of a mobile when the HTS-LNA front end is inserted along with  $X_0$  should provide a direct measure of the relative increase in cell loading  $\Delta X_0/X_0$  that can be

achieved. This, of course, assumes that the factor limiting network performance is associated with the reverse link.

In practice, the stochastic traffic associated with the varying number and spatial distribution of mobile users, the random nature of their usage, and the propagation characteristics of the region makes it desirable to go beyond an analytical analysis. Here, we have discussed a numerical simulation approach that allows us to address these concerns and to study the dynamic interplay of the reverse link and the forward link. In particular, it allows us to make a contact with and go beyond the analytical predictions concerning the effect of IMD noises on CDMA networks. This is an important feature of numerical simulations, because an IMD noise is frequently intermittent with an arbitrary time scale and spatially inhomogeneous making it difficult to obtain accurate analytical results in a general case.

The numerical simulations of the voice capacity increase associated with a reduction in the effective base-station receiver noise factor verified the analytical results for the relative increase in capacity utilization. The simulations also provided detailed information on how the instantaneous coverage areas and the soft-handoff regions changed when the normal front end of the base-station receiver was replaced by an HTS front end. A key finding from the simulations was the importance of properly optimizing the network in order to take advantage of the lower effective noise factor associated with the HTS front end. In particular, there is a need to increase the pilot and the forward-link transmission power to fully realize the HTS benefits.

#### ACKNOWLEDGMENT

The authors would like to thank R. Hammond, D. Chase, M. Eddy, N. Fenzi, J. Hamilton, and M. Williams for stimulating discussions.

#### REFERENCES

- [1] J. P. Simmons and J. M. Madden, "Practical HTS/cryogenic systems for wireless applications," *Microw. J.*, vol. 39, no. 10, pp. 124–136, Oct. 1996.
- [2] R. R. Conlon, "Superconductors do more with less," *Wireless Syst. Des.*, vol. 8, no. 6, p. 40, Jul./Aug. 2003.
- [3] M. I. Salkola, "CDMA capacity—Can you supersize that?" *Proc. IEEE Wireless Communications and Networking Conf.*, Orlando, FL, Mar. 17–21, 2002, vol. 2, p. 768.
- [4] J. S. Lee and L. E. Miller, *CDMA Systems Engineering Handbook*. Boston, MA: Artech House, 1998.
- [5] A. J. Viterbi, *CDMA: Principles of Spread Spectrum Communication*. Reading, MA: Addison-Wesley, 1995.
- [6] S. C. Yang, *CDMA RF System Engineering*. Boston, MA: Artech House, 1998.
- [7] N. Boucher, *Cellular Radio Handbook*. Mill Valey, CA: Quantum, 1992.
- [8] N. G. van Kampen, *Stochastic Processes in Physics and Chemistry*. Amsterdam, The Netherlands: North-Holland, 1981.

**M. I. Salkola** (M'06), photograph and biography not available at the time of publication.

**D. J. Scalapino**, photograph and biography not available at the time of publication.